Using Bearing-sensitive Infrared Sensor Arrays in Motion Localization for Human-following Robots

Yuebin Yang, Guodong Feng, Shaoxian Wang, Xuemei Guo, and Guoli Wang*
School of Information Science and Technology
Sun Yat-sen University, Guangzhou 510006, China
**isswgl@mail.sysu.edu.cn*

***Abstract*—This paper concerns the lightweight and robust infrared motion localization for human-following robots. We use bearing-sensitive pyroelectric infrared (PIR) sensor arrays in motion localization with two steps. The first step aims at generating bearing measurements of a human target from multiple perspectives with the PIR sensor arrays. The second step aims at locating the target through a least squares fusion of bearing measurements. The experimental results show that this approach ensures a human-following robot continuously working in an environment with complex background and light condition.**

I. Introduction

Human motion sensing is one of the most significant and fundamental technologies in human-robot interaction applications such as person location services and assisted living [1]-[2]. In robotics, various motion localization techniques have been proposed based on acoustic sensors, ultrasonic sensors, and optical imaging sensors for human localization. The applicability of acoustic [3] and ultrasonic [4] sensors is limited due to lacking of ability to distinguish the human target from other objects. For optical image sensors [5], the extraction of location information is highly sensitive to the light illumination and background changes.

In our previous work [6], we have proposed the concept of an infrared motion sensing system, as a lightweight and robust motion localization approach for human-following robots. The PIR sensor is of interest, because it is sensitive to the changes of infrared radiation induced by the human motion and robust to environmental changes [7]. The first prototype has been built as a proof-of-concept device, using multiple bearing-sensitive PIR sensor arrays with a modulation of the sensor field of view. The key to the location mechanism is the infrared cross-bearing localization techniques, for which we have done some researches in [8].

The primary contributions of this paper are the integrated design of above motion localization system for human-following robots, and validating whether this system is competent to a continuous following task in an environment with complex background and light condition. In order to test the system, we have simply defined a continuous following mechanism, and use the common Proportional-Integral-Derivative (PID) algorithm to control the paths of the robot. Knowing the performance of this motion localization system in the complex environment is useful for its application.

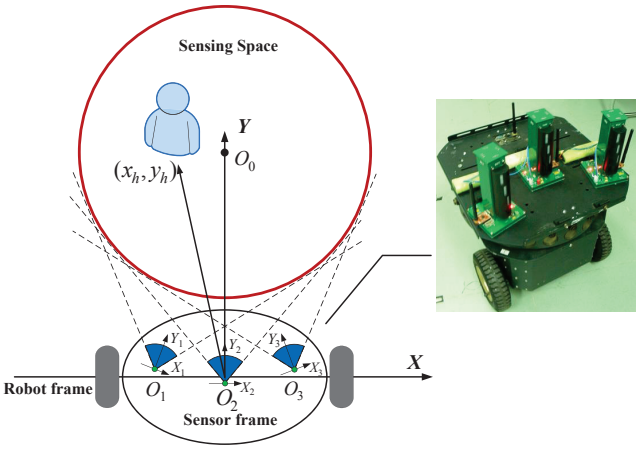

Fig. 1. Infrared motion sensing system: design model.

II. System Configuration

The following behavior of interest here is that the robot can follow a moving target person around but keep a certain distance to the target person. More specifically, consider the system model of a human-following robot as shown in Fig. 1. The coverage area of the human motion sensing system is modeled as a circle. The motivation of the human-following behaviors is to compensate for the motion of the target person shifting away from the center of the sensing coverage O_0.

It can be seen that human motion localization plays a crucial role in the above human-following task. This study will present a lightweight and robust sensing system for offering the motion cues in performing the above human-following task. In particular, we use multiple bearing sensitive PIR sensor arrays to organize this localization system. Obviously, when the bearing measurements from multiple perspectives are available, the motion location can be inferred based on the geometric correlations among the bearing measurements.

In order to describe the localization approach, we first define the coordinate frames of reference. As shown in Fig. 1, The robot frame is defined on the mobile robot. The origin of the robot frame is at the center of the mobile robot; the direction of the Y-axis is the robot's moving direction. The sensor frame is defined in the robot frame. The origin of the sensor frame is at the vertex of the entire field of view (FOV) of the PIR sensor array; the Y-axis vector is taken as the bisector vector

978-1-4673-5769-2/13/$31.00 ©2013 IEEE

of the entire FOV.

The new prototype after integrated design is shown in Fig. 1, which is mounted on the top deck of the mobile robot. The height of the robot is about 1m, and the sensing area of interest is centered at $O_0(0, 80\text{cm})$ with radius $r = 50\text{cm}$. The prototype consists of three bearing-sensitive PIR sensor arrays, and each sensor array consists of four PIR sensors placed in a vertical column. This structure contributes to the space saving of the top desk. Each PIR sensor in the sensor arrays associates a Fresnel lens. The PIR sensor and Fresnel lens used are D205B and 8719. The metallic masks are used to modulate the visibility of the sensors. Three PIR sensor arrays have the same FOV $\gamma = 4\pi/9$, and they see the sensing area from multiple perspectives. As shown in Fig. 1, the geometric constraint of the deployment is that the entire FOV of the PIR sensor array is the minimum fan-shaped envelop of the circular sensing area. From this, the deployment configuration parameters are chosen as $O_1(-17\text{cm}, 7\text{cm})$, $O_2(0, 0)$, $O_3(17\text{cm}, 7\text{cm})$. The logic behind such geometric constraint is to maximize the sensing coverage efficiency of a PIR sensor array.

III. Motion Localization

This section details how to use the bearing sensor arrays to locate a moving person. The motion localization consists of two steps: the bearing measurement and the date fusion.

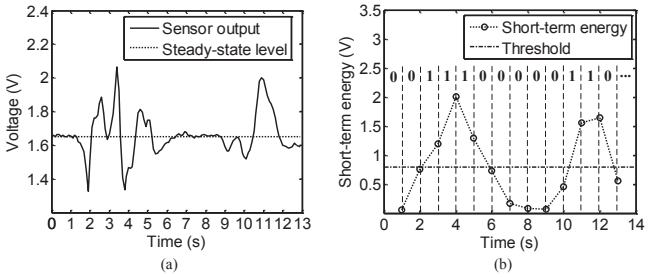

Fig. 2. The PIR sensor output signal and its processing. (a)The sensor output (b)The short-term energy of the signal and the thresholding.

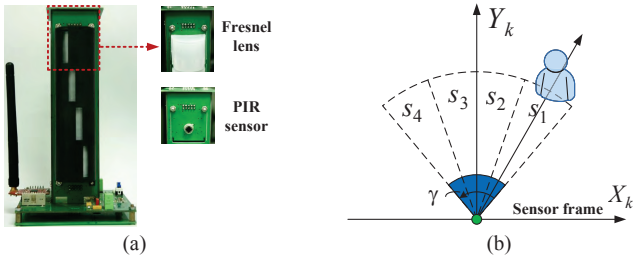

Fig. 3. A bearing-sensitive PIR sensor array. (a)Physical implementation (b)Sensor model.

A. Bearing Measurement

The bearing measurements is generate by the bearing-sensitive PIR sensor array. To this end, we use the PIR sensors as binary detectors, and the isomorphic bearing-sensitive visibility pattern is employed for visibility modulation.

Specifically, as an example, the amplified output signal of a PIR sensor is shown in Fig. 2(a). At $2s \sim 5s$, a human target is passing by the PIR sensor. At $6s \sim 8s$, the target keeps still, the PIR sensor is not triggered. The method of thresholding we used in our system has two stages as shown in Fig. 2(b). The first stage aims at calculating the short-term energy E of the analog sensor output x_t at present time t and the E is defined as

$$\mathrm{E} = \sum_{a=0}^{9} |x_{(t-a\Delta t)} - \mathrm{V}_s| \tag{1}$$

where the Δt means the sampling time and in this paper, $\Delta t = 100\text{ms}$ so as to match the motion pattern of a human target. The V_s is the steady state level and $\mathrm{V}_s = 1.65\text{V}$. The second stage produces the binary measurement of ith PIR sensor $\{m_i, i = 1, 2, 3, 4\}$ by

$$m_i = \begin{cases} 1 & : \quad \mathrm{E} \geq \lambda \\ 0 & : \quad \mathrm{E} < \lambda \end{cases} \tag{2}$$

where the λ means the threshold. From this, a binary sensor can effectively detect a person which occurs in its visible area.

In what follows, we can deploy the binary PIR sensors with the well modulated FOV to form a bearing-sensitive PIR sensor array. A bearing-sensitive PIR sensor array here consists of four planar co-located binary PIR sensors. The entire FOV of the PIR sensor array is segmented into a set of fan-shaped cells, each of which is visible only by one PIR sensor. In other words, there is one-to-one visibility correspondence between the fan-shaped cells and the PIR sensors. To build this one-to-one visibility correspondence, the FOV of each PIR sensor is required to be modulated to match with the corresponding cell. The required FOV modulation can be easily achieved by applying the bearing-sensitive visibility mask to the Fresnel lens arrays associated with the PIR sensors. The physical implementation of a sensor array is shown in Fig. 3(a).

With a bearing-sensitive PIR sensor array, the sensing model for generating the bearing measurements can be formulated as follows. We assume that the entire FOV of the PIR sensor array, γ ($\gamma < \pi$), is uniformly segmented into L (L=4 in this paper) fan-shaped cells. We will represent the sensing model in the sensor frame. We model the image of the entire FOV as the triggered state of the fan-shaped cells, defined as a vector $\mathbf{s} = [s_1, s_2, s_3, s_4]^{\mathrm{T}}$, where $s_l = 1$ if the infrared changes induced by human motion occur in the lth fan-shaped cell, otherwise $s_l = 0$. It is followed from the one-to-one correspondence of the bearing-sensitive PIR sensor array that the image $\mathbf{s}$ can be inferred directly from the binary PIR sensor outputs. Specifically, the value of s_l can be viewed as the binary quantization of the output of the lth PIR sensor m_l.

Consider the case that only one fan-shaped cell is triggered, for example, $s_l = 1$, the human motion is detected by lth PIR sensor. As shown in Fig. 3(b), the bearing measurement can be generated by $\varphi = \angle \mathbf{b}_l$, or

$$\varphi = \frac{\pi}{2} - \frac{(L + 1 - 2l)}{2L}\gamma \tag{3}$$

where $\mathbf{b}_l$ and $\angle\mathbf{b}_l$ denote the bisector vector of the lth fan-shaped cell and its angle to the positive X-axis, respectively. Obviously, two or more adjacent PIR sensors can be triggered simultaneously when the human motion occurs at the boundary of two adjacent cells, or the human motion covers multiple cells. For example, $n+1$ adjacent cells are triggered, that is, $s_j = 1$, $j = l, l+1, \cdots, l+n$. Then the bearing measurement can be generated by $\varphi = \angle\mathbf{b}_{l,n}$, that is

$$\varphi = \frac{\pi}{2} - \frac{(L+1-2l-n)}{2L}\gamma \tag{4}$$

where $\mathbf{b}_{l,n}$ denotes the angle bisector vector of the minimum envelop of the $n+1$ triggered cells. In this way, the bearing measurement can be unambiguously generated from the outputs of a bearing-sensitive PIR sensor array.

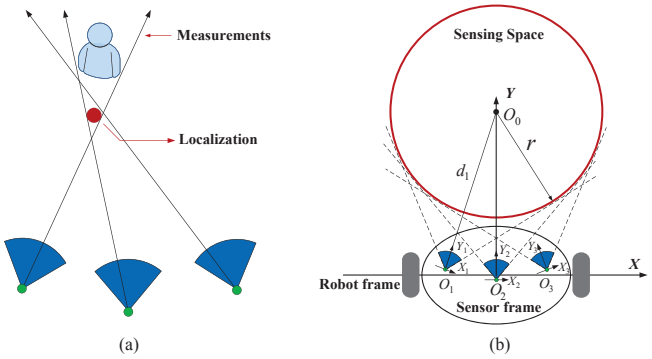

Fig. 4. The data fusion. (a)A schematic (b)Parameter definition.

B. Date Fusion

The design task here is to establish the fusion mechanism of the bearing measurements for inferring the human motion location. A schematic of data fusion is shown in Fig. 4(a). To this end, the least square method is used for data fusion.

In what follows, the human motion localization will be addressed in the robot frame. Firstly, the bearing measurement φ_k in the kth sensor frame should be transferred into robot frame. As shown in Fig. 4(b), based on the geometric constraints, we can get that for $k = 1, 2, 3$

$$\angle\overrightarrow{O_kO_0} = \alpha_k \tag{5}$$

and

$$\sin\gamma_k/2 = \frac{r}{d_k} \tag{6}$$

where $\angle\overrightarrow{O_kO_0}$ denotes the angle of the vector $\overrightarrow{O_kO_0}$ to the positive X-axis of the robot frame, d_k denotes the Euclidean distance between O_0 and O_k.

It can be seen that the bearing measurement φ_k in the kth sensor frame can be transferred into robot frame by

$$\beta_k = \varphi_k + \alpha_k - \pi/2 \tag{7}$$

That is, β_k given in Eq. (7) is the corresponding bearing measurement in the robot frame.

In what follows, we assume that the human motion occurs at P with coordinates (x_h, y_h). As mentioned above, the infrared changes due to the human motion will trigger one or more adjacent PIR sensors in the each PIR sensor array. Accordingly, the bearing measurements, $\{\beta_k, k = 1, 2, 3\}$, will be generated by the three PIR sensor arrays. The task of the cooperative sensing layer is to infer the human motion location P from the bearing measurements $\{\beta_k, k = 1, 2, 3\}$. This study focuses on finding the least square estimation P_e of P based on the cross-bearing correlations among the bearing measurements $\{\beta_k, k = 1, 2, 3\}$.

More specifically, as shown in Fig. 4(b), the human motion location P satisfies

$$\angle\overrightarrow{O_kP} = \beta_k \tag{8}$$

for $k = 1, 2, 3$. Eq. (8) can be equivalently represented as

$$(x_k - x)\sin\beta_k = (y_k - y)\cos\beta_k \tag{9}$$

Here (x_k, y_k) is the coordinate of O_k, $k = 1, 2, 3$. In matrix form, we have

$$\mathbf{Ap} = \mathbf{b} \tag{10}$$

where $\mathbf{p} = [x_h, y_h]^T$, $\mathbf{A}$ and $\mathbf{b}$ are given by

$$\mathbf{A} = \begin{bmatrix} \sin\beta_1 & -\cos\beta_1 \\ \sin\beta_2 & -\cos\beta_2 \\ \sin\beta_3 & -\cos\beta_3 \end{bmatrix}$$

$$\mathbf{b} = \begin{bmatrix} x_1\sin\beta_1 - y_1\cos\beta_1 \\ x_2\sin\beta_2 - y_2\cos\beta_2 \\ x_3\sin\beta_3 - y_3\cos\beta_3 \end{bmatrix}$$

Consequently, the least square estimation for $\mathbf{p}_e = [x_e, y_e]^T$ is given by

$$\mathbf{p}_e = (\mathbf{A}^T\mathbf{A})^{-1}\mathbf{A}^T\mathbf{b} \tag{11}$$

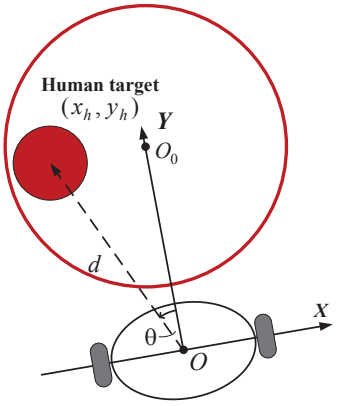

Fig. 5. Human following control.

IV. Human Following Control

In this paper, we want to validate whether this sensing system is competent to a continuous following task in the complex environment, especially in an environment with various light conditions. To this end, we will design a simple following controller so as to match the proposed localization system.

TABLE I
THE RESULTS OF THE HUMAN-LOCALIZATION EXPERIMENT.

No.	P (cm)	P_e (cm)	Error (cm)
1	(-40, 100)	(-32, 106)	10
2	(0, 80)	(0, 80)	0
3	(40, 100)	(45, 77)	24
4	(-40, 60)	(-25, 55)	16
5	(0, 60)	(0, 37)	23
6	(40, 60)	(28, 46)	18

Specifically, as shown in Fig. 5, when the motion localization information (x_h, y_h) is available, it will be firstly transferred into (θ, d). Thus, the motivation of the human-following behaviors can be formulated as: $\theta \to 0, d \to OO_0$. The O denotes the origin of the robot frame, and d denotes the Euclidean distance between O_0 and O. We use the common PID algorithm to control the following behaviors. More specifically, the inputs of the controller are (θ, d), and the outputs are (v, w), where v denotes the linear velocity and w denotes the angular speed. The adjustment of the parameter θ is a high-priority task, and the θ decides the w through the PID algorithm. During the adjustment of θ, the $v = 0$. Only when the θ is lower than a threshold, the $\Delta d = d - OO_0$ will be used to decide the v, and the w will be set into 0.

Fig. 6. Snapshots of the human-localization experiment. (a)Moving in (40, 100) (b)Moving in (-40, 100) (c)Moving in (-40, 60).

V. EXPERIMENT AND DISCUSSION

In what follows, two experiments, the human motion localization and the human-following task, are conducted to evaluate the developed system prototype. Moveover, some discussions will be given based on the experimental results.

A. Experimental Studies

The procedures of the human-localization experiment can be summarized as follows. Firstly, the target person activated the normal walking movement within the sensing area so as to induce the infrared radiation changes at the specified location. Then, the outputs of the PIR sensors were collected to generate the bearing measurements. Finally, with the bearing measurements were available, and the human motion location was estimated by the least square method. The snapshots of the human-localization experiment are shown in Fig. 6. The experimental results are listed in Table I. It can be observed that the localization errors in the sensing area are less than 30cm, which is practically acceptable for the human following tasks.

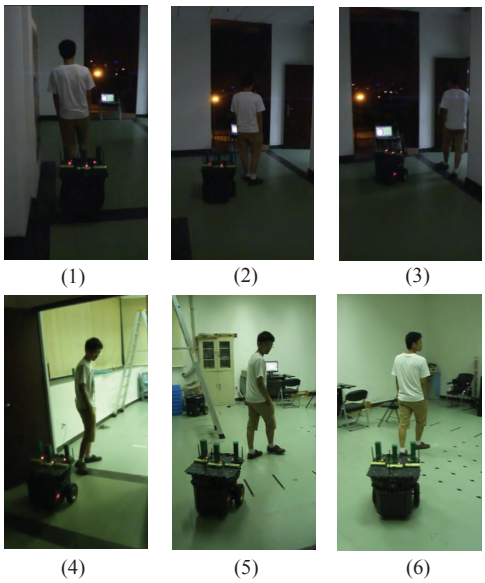

Fig. 7. Snapshots of the human-following experiment.

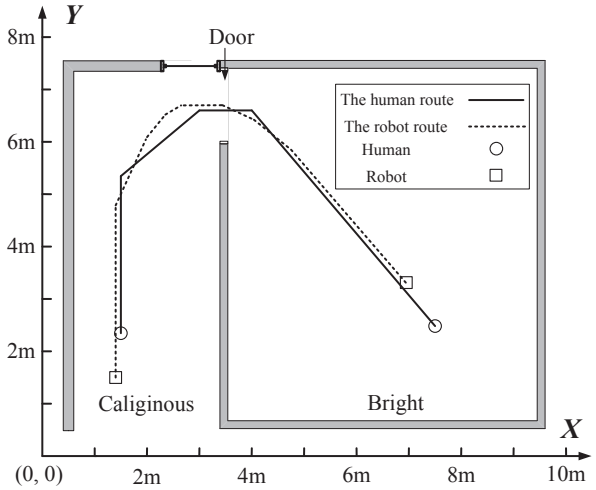

Fig. 8. The results of the human-following experiment.

Furthermore, we want to validate whether the system is competent to a continuous following task in an environment with complex background and light condition. To this end, a human-following experiment is conducted in an obstacle-free environment with size of 10m×8m. The target person to be followed is asked to walk normally along the predefined route. The experiment begins in a caliginous corridor, and the destination is a bright room. As shown in Fig. 8 (solid line), the predefined route is composed of four line segments. The average walking speed is required to be kept at roughly 0.4m/s. The moving speed and direction are decided by the human following controller which is discussed above. The parameters of the PID algorithm must be preset by experiment, so as to match with the motion pattern of the target person. The snapshots of the experimental environment are shown in Fig. 7. From the Fig. 7, we can see the background of the

experimental environment is complex.

We set the global frame as in Fig. 8. The robot is initially located at $(1.5\text{m}, 1.5\text{m})$, and the target person starts walking from the center O_0 of the sensing area. The following route of the robot measured manually is plotted in Fig. 8. It can be observed that the errors of the human motion localization can be kept at an acceptable level to facilitate the human-following task.

B. Discussion

From the experimental results, we can see that the proposed localization system is competent to a continuous following task in the complex environment. Other advantages of this PIR sensor based system include low-cost and low-power. A disadvantage of this location approach is: the bearing measurements inevitably have a time delay due to the slow response time of the PIR sensor and the method of thresholding. For this reason, multi-sensor fusion techniques can be used to further improve the performance of the proposed system. On the other hand, the proposed infrared localization system achieves low dataloads but have poor spatial resolution. More precisely, the generation of the bearing measurements is a quantization process and can inevitably result in the quantization errors. The larger the number of PIR sensors is, the smaller the quantization errors are. However, the increasing of the sensor number will lead to the decreasing of the visible area. In this situation, the sensibility of the system will become an important consideration.

In addition, more sophisticated human-following algorithms can be developed so as to achieve a better following performance. Nevertheless, this work is beyond the scope of this paper, and some relative works can be found in [9] and [10]. How to integrate existing navigation algorithms into the proposed sensing system may be a meaningful but challenging work.

VI. Conclusion

This paper focuses on the integrated design of the motion localization system for the human following robots using bearing-sensitive PIR sensor arrays. The proposed localization system could directly generate the bearing measurements of the moving target, which is lightweight and robust to the environmental changes. The target is localized through fusing the bearing measurements from multiple perspectives with the least squares method, which does not involve complex computation. Hence, the proposed infrared motion sensing system has prominent advantages in the mobile sensing applications.

In the future work, we will extend this study in two aspects: 1) using more exquisite fusion mechanism such as Bayesian filter to synthesize the bearing measurements from multiple perspectives, and 2) developing much sophisticated human-following algorithms.

Acknowledgment

This work was partly supported by the National Nature Science Foundation under Grant 61074167.

References

[1] L. Atallahand and G. Z. Yang (2009). "The use of pervasive sensing for behaviour profiling–a survey," *Pervasive and Mobile Computing*, vol. 5, no. 5, pp. 447-464, 2009.

[2] A.Jaimes and N. Sebe, "Multimodal human-computer interaction: A survey," *Computer Vision and Image Understanding*, vol. 108, no. 1-2, pp. 116-134, 2007.

[3] A, Sekmen, M. Wilkes, and K. Kawamura, "An application of passive human-robot interaction: human tracking based on attention distraction," *IEEE Trans.Syst, Man, Cybern.A, Syst.Humans*, vol. 32, no. 2, pp. 248-259, 2002.

[4] F. Tong, S. Tso, and T. Xu, "A high precision ultrasonic docking system used for automatic guided vehicle," *Sensors and Actuators A: Physical*, vol. 118, no. 2, pp. 183-189, 2005.

[5] Q. Cai, and J.K. Aggarwal, "Tracking human motion in structured environments using a distributed-camera system," *Pattern Analysis and Machine Intelligence, IEEE Transactions on* , vol.21, no.11, pp.1241-1247, Nov. 1999.

[6] G. D. Feng, X. M. Guo and G. L. Wang, "Infrared Motion Sensing System for Human-following Robots," *Sensors & Actuators: A. Physical*, Vol. 186, 2012.

[7] A. Hossain and M. Rashid, "Pyroelectric detectors and their applications," *IEEE Trans. Industry Applications*, vol. 27, no. 5, pp. 824-829, 1991.

[8] Y. B. Yang, G. D. Feng, X. M. Guo and G. L. Wang, "Compressed Infrared Bearing-sensor for Human Localization: Design and Implementation," *IEEE International Conference on Information and Automation*, Shenyang, China, June. 6-8, 2012.

[9] K. Morioka, J.-H. Lee and H. Hashimoto, "Human-following mobile robot in a distributed intelligent sensor network," *Industrial Electronics, IEEE Transactions on*, vol.51, no.1, pp. 229- 237, Feb. 2004.

[10] I. R. Manchester, E.-M.P. Low and A. V. Savkin, "Interception of a moving object with a specified approach angle by a wheeled robot," *47th IEEE International Conference on Decision and Control*, Mexico, pp. 490-495, Dec. 2008.